

# High Power, Wideband Single Crystal XBAW Technology for sub-6 GHz Micro RF Filter Applications

Ramakrishna Vetury  
Akoustis Technologies  
Huntersville, NC  
USA

Michael D. Hodge  
Akoustis Technologies  
Huntersville, NC  
USA

Jeffrey B. Shealy  
Akoustis Technologies  
Huntersville, NC  
USA

**Abstract**—The authors report a Bulk Acoustic Wave (BAW) filter technology built using a 6-inch MEMS wafer process on a Si substrate, compatible with single crystal and polycrystalline aluminum nitride (AlN) piezoelectric materials (denoted as XBAW), and present metrics demonstrating resonator technology capable of highly reliable, high power, compact, high performance RF filter solutions in the sub-6 GHz spectrum, with proven high  $Q_{max}$  of 3685 and resonator Figure-Of-Merit (FOM) of 222 at 1.8GHz. Using the XBAW process, the authors compare power handling capability of filters built from single crystal Metal-Organic Chemical Vapor Deposition (MOCVD) AlN and polycrystalline Physical Vapor Deposition (PVD) AlN piezoelectric materials, showing that power handling capability of single crystal MOCVD AlN XBAW technology exceeds PVD AlN XBAW by 2.3x, when packaged and by 1.8x, when measured on-wafer. A first reliability study shows that survival times of single crystal MOCVD AlN XBAW filters far exceed survival times of PVD-AlN XBAW filters. As an example of high frequency capability, the authors report filters with a center frequency of 5.25 GHz, a 3dB bandwidth of 205 MHz, a minimum insertion loss of 0.83dB, excellent wide band rejection from 30 MHz to 11 GHz and attenuation greater than 50dB in the UNII 2C+3 bands.

**Index Terms**—RF Filters, Mobile communication, Piezoelectric devices, Electromechanical devices, Wide band gap semiconductors, bulk acoustic wave resonators, UNII, acoustic filters, BAW filters, WiFi.

## I. INTRODUCTION

Broadband and high data rate transmission is leading to the emergence of new Wi-Fi bands and cellular bands in the sub-6 GHz spectrum [1]. Tri-band routers delivering to IEEE 802.11ac standard transmit at 2.4 GHz and two bands in 5-6 GHz spectrum. Current routers support UNII 1+2A and UNII 2E+3 bands and require small form factor coexistent filters above 5 GHz. Besides the growth of higher frequency Wi-Fi applications, emerging LTE/cellular bands in the sub-6 GHz spectrum require next generation wireless infrastructure. Infrastructure applications require filters capable of higher power handling capability than handset applications, plus capability to support multiple bands, complex architectures (carrier aggregation, diversity and Multiple Inputs Multiple Outputs (MIMO)), plus low insertion loss, high out of band rejection and excellent linearity. All these requirements must

be achieved in small form factors demanded by next generation phased array architectures.

Incumbent acoustic filter technologies are based on surface acoustic wave (SAW) and BAW resonators. Frequencies greater than 3 GHz are challenging for SAW RF filters due to small width and pitch required of the interdigitated fingers [2], which has led to the dominance of BAW acoustic filters for higher frequencies.

Film bulk acoustic resonator (FBAR) [3] and solidly mounted resonators (SMR) [4] are the dominant BAW resonator technologies utilized in RF filters due to their compact size. Currently, FBAR and SMR BAW resonators are constructed by depositing piezo-electric AlN thin films via PVD techniques such as sputter deposition. The resulting PVD AlN thin films are poly-crystalline, while MOCVD deposited AlN thin films are single crystals. In this work, the authors demonstrate that a unique combination of high thermal conductivity and excellent piezo-electric properties allows the creation of a new class of high power BAW RF filters (XBAW) in the sub-6GHz spectrum.

## II. MATERIALS

Single crystal epitaxial piezoelectric layers were grown via conventional MOCVD. Full-width half-maximum (FWHM) of (0002) X-ray diffraction (XRD) rocking curve was used to assess crystal quality. FWHM of MOCVD AlN films was  $0.03^\circ$ , compared to typical FWHM of  $2-3^\circ$  in PVD AlN.

Simulations have suggested that the lateral heat conduction of poly-Si films is significantly lower than single crystal Si thin films and that lateral heat conduction in poly-Si films does not increase with increasing thickness, in contrast to improvement in lateral heat conductivity of single crystal Si films with increasing thickness [5]. It has been reported that thermal conductivity of polycrystalline AlN thin films degrades as film thickness decreases [6]. In addition, improved crystal quality in the single crystal AlN has been demonstrated to result in improvements in acoustic velocity [7] and potentially improved piezoelectric coefficients [8]. A higher longitudinal acoustic velocity in AlN piezo-material allows for thicker AlN and thicker electrode metal for the same frequency.

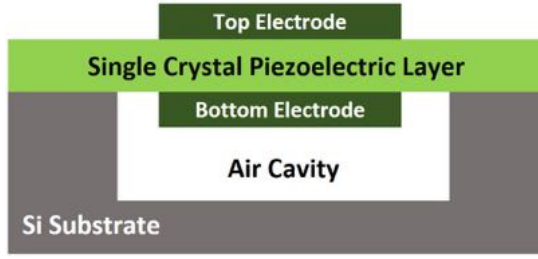


Fig. 1. A diagram of the fabricated resonators, illustrating top and bottom electrodes on single crystal AlN situated inside a Si substrate cavity.

These factors improve the thermal conduction pathway from the resonator to the heatsink, suggesting that single crystal MOCVD AlN can improve power handling capability of BAW filters.

### III. DEVICE TECHNOLOGY

Table 1 summarizes prior work [9]–[13] and demonstrated results using both PVD-AlN and single crystal MOCVD Group III-Nitride BAW resonators [14]–[18].

TABLE I  
SINGLE CRYSTAL GROUP III-NITRIDE BULK ACOUSTIC RESONATORS

Ref.	XRD	Stack	Freq (GHz)	$k_{eff}^2$ (%)	$Q_{max}$	FOM
[14]	–	GaN/AlN	1.1	5.0	–	–
[15]	0.23°	GaN	6.3	3.4	*1130	38
[16]	0.36°	GaN	2.1	–	*424	–
[17]	2.4°	AlN	3.7	1.1	*1557	17
[18]	0.37°	AlGaN	2.3	4.44	1277	57
[19]	0.025°	AlN	3.8	7.63	858	66
[19]	0.025°	AlN	3.8	5.87	1572	92
[20]	0.027°	AlN	5.2	6.32	1523	96
This work	0.03°	AlN	1.8	6.03	3685	222
This work	0.03°	AlN	3.8	6.30	2589	163
This work	0.03°	AlN	5.2	6.26	2136	134

\*In this work, Q-factor is calculated from the full mBVD model following [21]. Note [15] [16] [17] quote  $Q_r$  which uses only the motional arm of the mBVD model.

In this work, filters were fabricated using MOCVD and PVD AlN with nominal 0.5  $\mu\text{m}$  thickness, processed in the same MEMS-based wafer fabrication process on 6-inch Si substrates (XBAW), enabling a direct comparison of MOCVD AlN and PVD AlN materials. The wafer process included sputter-deposited electrode metals and resulted in resonators with two air interfaces and backside electrodes routed to the top side of wafer by vias in the AlN layer. A simplified representation of the structure of fabricated resonators is shown in Fig. 1.

### IV. RESONATOR CHARACTERISTICS

On-wafer, air coplanar probe S-parameter measurement of 1-port 50ohm resonators was followed by de-embedding of manifold elements between the intrinsic resonator and the measurement probe plane to obtain intrinsic resonator characteristics. Intrinsic resonator data, including Smith chart plots of the reflection coefficient i.e. "Q-circle" and the dependence of Q on frequency i.e. "Bode Q-Plot" for representative 50

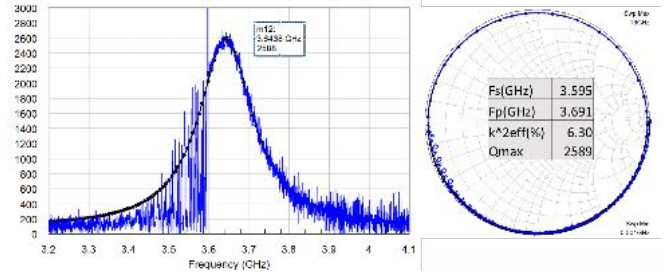


Fig. 2. "Q-circle" and "Bode Q-Plot" for representative 50 ohm XBAW resonators at 3.8GHz

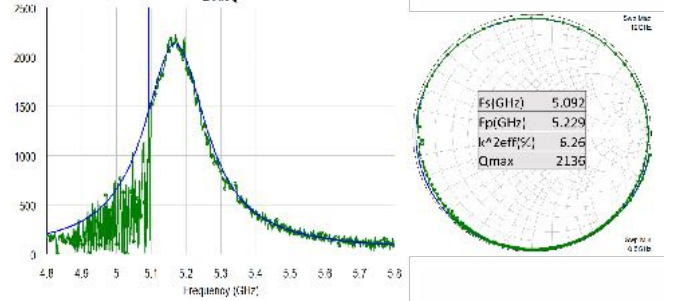


Fig. 3. "Q-circle" and "Bode Q-Plot" for representative 50 ohm XBAW resonators at 5.2 GHz

ohm resonators at 3.8 GHz and 5.2 GHz is shown in Figs. 2 and 3.

The measured and de-embedded data was fit to a modified Butterworth Van-Dyke (mBVD) model. The mBVD model parameters were obtained by simultaneously optimizing fit to measured S and Y parameters and "Bode Q-Plot", as previously reported by authors [19]. As is seen in Figs. 2 and 3, excellent agreement is obtained between measured data and mBVD model. A resonant frequency ( $f_s$ ) and an anti-resonant frequency ( $f_p$ ) are extracted from the zero crossing of phase of the de-embedded resonator Y-parameters.  $k_{eff}^2$  is calculated using eq. (1) and Q-factor was evaluated using the method described in [21], consistent with previous work by authors [19]. A resonator figure of merit (FOM)  $Q_{max}.k_{eff}^2$  was calculated at 1.8 GHz, 3.8 GHz and 5.2 GHz.

$$k_{eff}^2 = \frac{\pi^2}{4} \cdot \frac{f_1}{f_2} \cdot \frac{f_2 - f_1}{f_2} \quad (1)$$

$$Q(\omega) = \omega \frac{d\phi}{d\omega} \frac{|S_{11}|}{1 - |S_{11}|^2} \quad (2)$$

Fig. 4 summarizes the key technology metrics over frequency, demonstrating the capability of XBAW as an enabling technology for sub-6 GHz RF filter solutions with proven high  $Q_{max}$  of 3685 and resonator FOM of 222 at 1.8GHz.

### V. FILTER PERFORMANCE

A ladder network filter was designed using a modified (to include resistances) Mason resonator model. A comparison of measured filter performance versus reported BAW based 5.2 GHz filters is shown in Table II. A plot of the measured

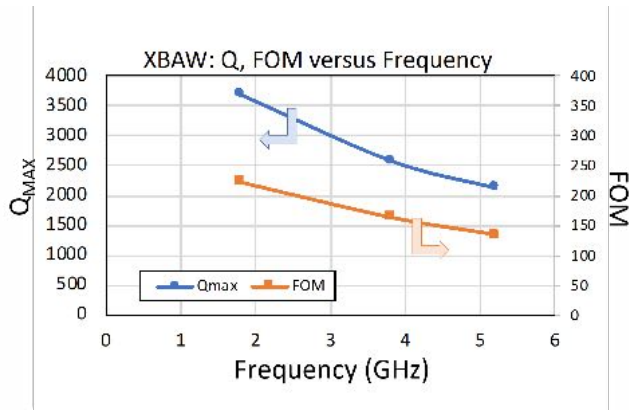


Fig. 4. Plot showing the key technology metrics over frequency, demonstrating the capability of XBAW as an enabling technology for sub-6 GHz RF filter solutions with proven high  $Q_{max}$  of 3685 and resonator FOM of 222 at 1.8GHz.

TABLE II  
HIGH PERFORMANCE 5.2GHz BULK ACOUSTIC WAVE FILTERS

Ref.	Stages	Reject (dB)	Mean IL (dB)	4dB BW (MHz)
[11]	4	20	$\approx 1.8$	$>230$
[13]	3.5	25	$\approx 2.5$	170
This work	4.5	$>50$	1	205

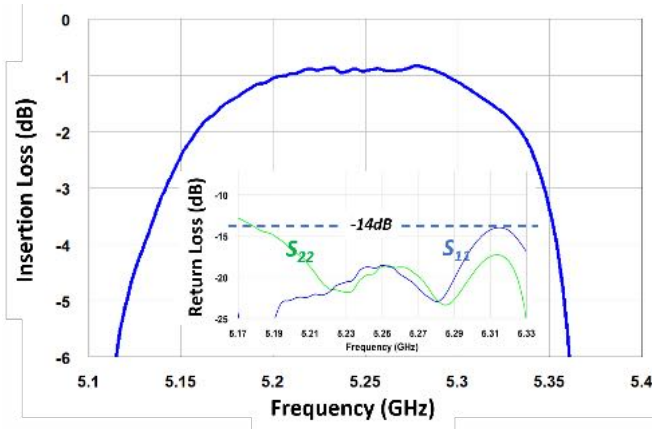


Fig. 5. Measured narrow band  $S_{21}$  performance of 5.25 GHz packaged filter, showing minimum IL of 0.83 dB, an average IL of 1.1 dB and 205 MHz of 3dB bandwidth.

filter passband response is shown in Fig. 5, demonstrating a minimum IL of 0.86 dB, an average IL of 1 dB, center frequency of 5.25 GHz, and an absolute 3 dB bandwidth of 205 MHz. A wide band plot of the filter performance ( $S_{21}$ ) is shown in Fig. 6 and shows out of band rejection better than 50dB in the UNI-2E/C/3/4 band.

## VI. POWER HANDLING AND INITIAL RELIABILITY

A comparison of power handling of single crystal MOCVD-AIN XBAW and polycrystalline PVD-AIN XBAW technology, using the same XBAW wafer fabrication process was conducted using measurements of power handling. Measurements were conducted on die mounted on laminates as well as on-

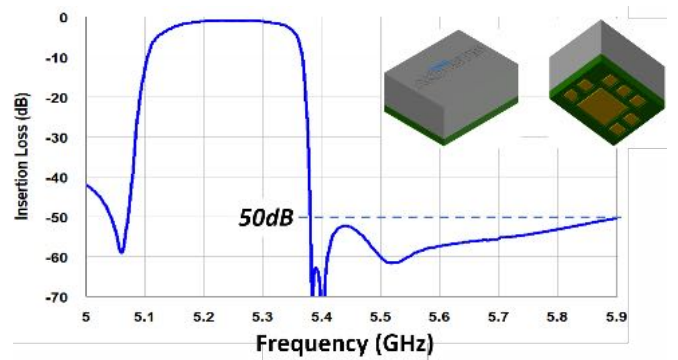


Fig. 6. Wide band plot of measured packaged filter performance ( $S_{21}$ ), showing rejection better than 50dB in the UNI-2E/C/3/4 band.

wafer. Using a 10% duty cycle WCDMA signal, the input power was linearly increased in steps of 0.5dB and the average output power was measured (using a power meter) to evaluate changes in resonator insertion loss. Single crystal MOCVD-AIN XBAW technology consistently showed improvement in maximum input power sustained before catastrophic failure as shown in Fig. 7. The average improvement in power handling, for die mounted on laminate, was 3.7dB, i.e. a 2.3x improvement in power over polycrystalline PVD AIN XBAW technology and the average improvement in power handling, measured on-wafer, was 2.9dB, i.e. a 1.95x improvement in power handling over polycrystalline PVD AIN XBAW technology.

Time-to-failure (TTF) of single crystal MOCVD AIN and PVD AIN based filters, constructed using the same wafer fabrication process was measured using a 10% duty cycle WCDMA signal. The input power was held constant at power levels appropriately backed off from the point of catastrophic failure, and output power was measured to evaluate resonator insertion loss and the time at which catastrophic damage occurred in the device. TTF was defined as the time at which the insertion loss degraded by  $>1$ dB. The same test filter was used as a vehicle to compare technologies. Survival times from this study were compared with reported TTF data [22] as shown in Fig. 8. This figure shows that for similar input power levels, single crystal MOCVD-AIN XBAW technology has significantly longer TTF than polycrystalline PVD AIN XBAW technology.

It is noted that the same simple ladder network filter was used in both studies, and no circuit or architecture enhancements to increase either power handling or TTF were deployed.

## VII. CONCLUSION

In this work, the authors demonstrate a unique combination of materials with high thermal conductivity and excellent piezo-electric properties, utilizing a MEMs 6-inch Si substrate wafer process, creating a new high power XBAW RF filter technology in the sub-6 GHz spectrum with proven high  $Q_{max}$  of 3685 and resonator FOM of 222 at 1.8 GHz.

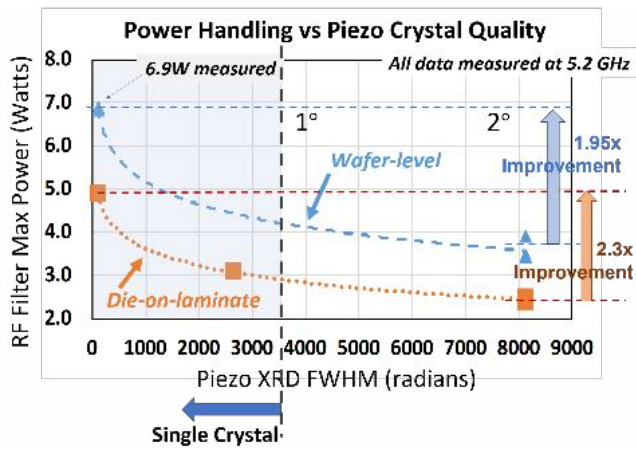


Fig. 7. Measured power handling capability at 5.2 GHz of single crystal MOCVD AlN XBAW technology exceeds PVD AlN XBAW technology by 2.3x when comparing die mounted on laminate and by 1.95x when comparing die tested on-wafer.

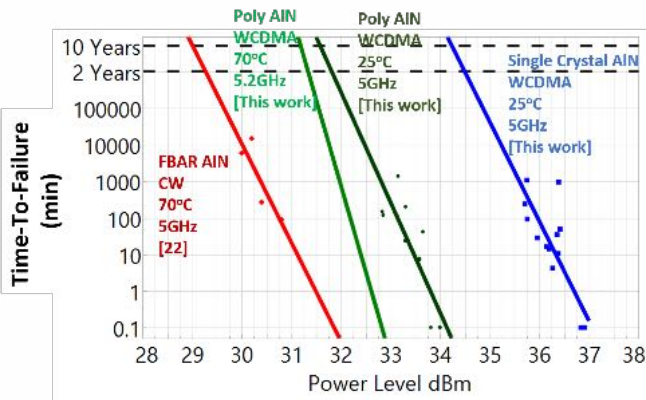


Fig. 8. A direct comparison of single crystal MOCVD AlN XBAW technology and polycrystalline PVD AlN XBAW technology, shows significantly longer survival times for MOCVD AlN XBAW technology, using packaged, simple ladder network filters that are fabricated in same XBAW process and measured at 5.2 GHz

Using the XBAW process, the authors compare power handling capability of filters built from single crystal MOCVD AlN and PVD AlN piezoelectric materials, showing that power handling capability of single crystal MOCVD AlN XBAW technology exceeds PVD AlN XBAW by 2.3x, when packaged and by 1.8x, when measured on-wafer. A first reliability study shows that survival times of single crystal MOCVD AlN XBAW filters far exceed survival times of PVD-AlN XBAW filters. As an example of high frequency capability, the authors report filters with a center frequency of 5.25 GHz, a 3dB bandwidth of 205 MHz, a minimum insertion loss of 0.83dB, excellent wide band rejection from 30 MHz to 11 GHz and attenuation greater than 50dB in the UNI-2C/E/3/4 band.

#### REFERENCES

[1] <http://www.networkcomputing.com/wireless/channel-bonding-wifi-rules-and-regulations/199326059>  
 [2] K. Hashimoto, "RF Bulk Acoustic Wave Filters for Communications" Artech House., pp161-171, 2009

[3] R. Ruby, "Current Status, Future Growth for Filters used in Cell Phones...", *Proc. Intl Symp. on Acoustic Devices*, Chiba, Japan, 2015, pp13-17.  
 [4] R. Aigner et al., "The Edge of Tomorrow in BAW: Innovate, Ramp, Repeat.", *Proc. Intl Symp. on Acoustic Devices*, Chiba, Japan, 2015, pp7-12.  
 [5] S. Ju, X. Liang and X. Xu, "Out-of-plane thermal conductivity of polycrystalline silicon nanofilm by molecular dynamics simulation" *Jo. of Applied Physics*, 110(5), pp054318-054318, 2011  
 [6] S.R.Choi, "Thermal Conductivity of AlN and SiC Thin Films" *Int. Jo. of Thermophys.*, p896, 2006  
 [7] S.R. Gibb, et al., "Single Crystal AlN Films With Improved Elastic and Piezoelectric Properties for Bulk Acoustic Wave Filters," *International Conference on Nitride Semiconductors*, Strasbourg, France, July 24-28th, 2017  
 [8] Y. Ohashi, M.Arakawa, J. Kushibiki, B. Epelbaum, A. Winnacker., Ultrasonic Microscopy Characterization of AlN Single Crystals *Appl. Phys. Express*. 077004 p1-3, 2008.  
 [9] K.M. Lakin, J.R. Belsick, J.P. McDonald, K.T. McCarron, C.W. Andrus, "Thin Film Resonators and Filters, in *Micr. Symp. Digest, IEEE IMS.*, pp1487-1490, 2002.  
 [10] H.P. Loebel, C. Metzmacher, D.N. Peligrad, "Solidly mounted bulk acoustic wavefilters for the GHz frequency range, in *Proc. IEEE Ultrason. Symp.*, pp919-923, 2002.  
 [11] T. Nishihara, T. Yokoyama, T. Miyashita, and Y. Satoh, "High performance and miniature thin film bulk acoustic wave filters for 5 GHz, *Proc. IEEE Ultrason. Symp.*, pp969-972, 2002.  
 [12] R. Lanz, P. Murali, "Solidly mounted BAW filters for 8 GHz based on AlN thin films, *Proc. IEEE Ultrason. Symp.*, pp178-181, 2003.  
 [13] G.G. Fattinger, J. Kaitila, R. Aigner, W.Nessler, "Thin Film Bulk Acoustic Wave Devices for Applications at 5.2GHz," *Proc. IEEE Ultrasonics Symposium*, p174, 2003  
 [14] K. Mutamba, D. Neculoiu, A. Muller, G. Konstantinidis, "Micromachined GaN-based FBAR Structures for Microwave Applications, *Proc. of Asia-Pacific Microwave Conf.*, 2006.  
 [15] A. Muller, et. Al., "6.3GHz FBAR Structures Based upon Gallium Nitride/Silicon Thin Membrane, *IEEE Elec. Dev. Lett.*, Vol. 30, No. 8, pp799-801, 2009.  
 [16] M. Rais-Zadeh, V. J. Gokhale, A. Ansari, "Gallium Nitride as an Electromechanical Material, *Jour. Micro. Sys.* 23 (6), Dec. 2014.  
 [17] Y. Aota, et al., "Fabrication of FBAR for GHz Band Pass Filter with AlN Film grown by MOCVD, in *Proc. IEEE Ultrason. Symp.*, pp337-338, 2006.  
 [18] J.B. Shealy, M.D. Hodge, P. Patel, "Single Crystal AlGaIn Bulk Acoustic Wave Resonators on Silicon Substrates with High Electromechanical Coupling," *IEEE Radio Frequency Integrated Circuits Symposium*, May 22-24, 2016  
 [19] J.B. Shealy, et al., "Low Loss, 3.7GHz Wideband BAW Filters, Using High Power Single Crystal AlN-on-SiC Resonators," *IEEE International Microwave Symposium*, June 2016.  
 [20] M.D. Hodge et al., "High Rejection UNII 5.2GHz Wideband Bulk Acoustic Wave Filters Using Undoped Single Crystal AlN-on-SiC Resonators," *IEEE International Electron Devices Meeting*, Dec 2017.  
 [21] R. Ruby, R. Parker, D. Feld, "Method of Extracting Unloaded Q Applied Across Different Resonator Technologies, *Proc. of IEEE Ultrason. Symp.*, pp1815-1818, 2008  
 [22] Y. Satoh, T. Nishihara, T. Yokoyama, M. Ueda and T. Miyashita, *Jpn. J. Appl. Phys.*, v44, p2883, 2005.